Geotechnical Engineering in the XXI Century: Lessons learned and future challenges
N.P. López-Acosta et al. (Eds.)

doi:10.3233/STAL190090

Determination and Comparison of the N'q Factor of Pile Capacity

Sergio Antonio MARTÍNEZ-GALVÁN[a,1], Neftalí SARMIENTO-SOLANO[a] and Juan Fernando TOVAR-FLORES[b]
[a] *Instituto Politécnico Nacional, Profesor SEPI, ESIA UZ, México*
[b] *Instituto Politécnico Nacional, Postgraduate, SEPI, ESIA UZ, México. Geotechnical coordinator, LIEC SA de CV, Mexico*

Abstract. The present article disseminates the evaluation of the N'_q factor to calculate tip load capacity of individual piles, obviously as a function of the internal friction angle of the support soil of the pile tip. The evaluation of the factor is by means of numerical analysis with the finite element method. The numerical model considers the pile axisymmetric geometry, the pile embedding in a granular deposit and pile-soil interface. The pile is modeled with solid elements and linear elastic behavior. The analysis considers a single hypothetical stratigraphy: cohesive soil 12 m thick, which overlies granular material. The behavior of the soils is elastoplastic with Mohr-Coulomb failure criterion. The parameters of soil strength are: a) cohesive soil, cohesion of 50.0 kPa and zero internal friction angle; b) granular soil, zero cohesion and internal friction angle variable between 25 to 45 degrees. The objective of this study is to determine the influence of the resistance of the supporting soil on the magnitude of the N'_q factor and to compare the calculated factor with previous solutions commonly used in the geotechnical design of piles. The proposed factor is the result of a parametric-numerical analysis, where prior to the evaluation of the N'_q factor, the influence of the effective embedment depth is considered.

Keywords. Single pile, bearing capacity, numerical method, failure mechanism.

1. Introduction

Combining the techniques of the finite element method and the superior theorem of the theory of plasticity, it generates a powerful tool to evaluate mainly stability problems and in particular to determine collapse loads or failure mechanisms [1-3].

The general use of foundation piles is to save weak soil strata, to support the pile in a hard soil deposit (cohesive-frictional soils). The transfer mechanism of pile load to the subsoil is by shaft and by tip, Figure 1b [4]. The choice of pile length (L) depends mainly on the depth at which the hard ground is, the pile diameter predefined (D), of the load applied by the superstructure, of soil strength that confines the pile and of soil located in pile tip. Another variable that affects the resistance offered by the pile is the effective embedment depth (L_b) in the hard soil deposit, Figure 1b.

Figure 1a (pile head curve) shows the load-displacement curve of a full-scale test of an isolated pile with axial load applied on pile head, described by [4] as a curve with three parts. To point A, the main contribution of resistance pile is by shaft; in A-B section,

[1] samartinezg@ipn.mx o sergio.mtz.g.per@gmail.com.

both resistances shaft and tip, offer resistance to pile penetration; and in B-C section only pile tip offers resistance and whole shaft is plasticized by shear stresses. By separating this behavior, tip and shaft curves show both contributions.

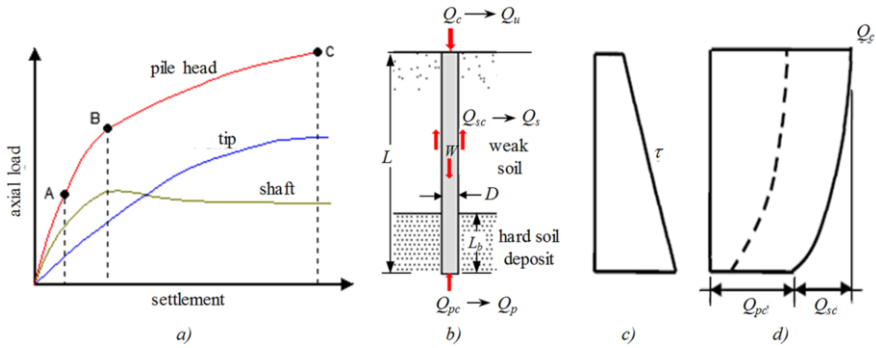

Figure 1. Individual pile behavior. Modified from [4].

The transfer of axial load applied in pile head (Q_c) to the subsoil, is through the pile-soil interaction, in generation order, first the pile shaft resistance (Q_{sc}) that develops the adjacent soil to the pile and then, the resistance to the pile tip penetration (Q_{pc}) offered by support soil, the own weight (W) of the same pile increases the axial load, Figure 1b. By shaft and by tip, subsoil shear strength (τ, Figure 1c) counteracts the axial load. For any Q_c magnitude, including the collapse load (Q_u), the magnitudes Q_{sc} and Q_{pc} vary, Figure 1d shows the distribution of the shaft and tip resistance offered by the pile.

Due to the pile-soil load transfer, when relative Q_c occurs, relative displacements occur in the pile-soil lateral interface, which activate shaft resistance. For $Q_c = Q_A$ (point A of Figure 1a), the resistance distribution by shaft and tip is indicated by the dotted curve of Figure 1d, the load transferred to the tip is small. By increasing Q_c to point B, all resistance per shaft is mobilized and any increased load is taken only by the tip of the pile. By increasing Q_c to point C, only the resistance at the tip is mobilized and load transfer is indicated by the solid line of Figure 1d. In the load interval from B to C, the resistance in the shaft remains constant.

To load collapse: Q_c, Q_{sc} and Q_{pc} tend respectively to ultimate load capacity (Q_u), ultimate shaft capacity (Q_s) and ultimate tip capacity (Q_p). For a single pile [5], Q_u is:

$$Q_u = Q_p + Q_s \tag{1}$$

$$Q_s = \sum_{i=1}^{n} (c_{ui} L_i) \propto \pi D \tag{2}$$

$$Q_p = (c_u N_c' + q N'_q + 0.5 \gamma D N'_\gamma) A_s \tag{3}$$

where c_{ui} is undrained cohesion of the strata that covers the length of the pile (L); α is a parameter that reduces the soil resistance due to the soil remolding generated by the pile construction (cast-in-place concrete piles); implicitly, A_f is pile shaft area (= πDL); c_u is undrained cohesion of tip pile soil; q is effective vertical stress at tip pile level, $q = \gamma D_f$; γ is effective volumetric weight of tip pile soil; D_f is effective embedment depth; D is pile diameter; N'_c, N'_q and N'_γ are load capacity factors due respectively to cohesion, to

overload by pile soil adjacent and to weight of tip pile soil and; A_s is pile section area (= π $D^2/4$). Note that $D_f \neq L_b$, see Figure 5a.

To circular pile and cohesive soil, $N'_c = 9$. In practice, the pile diameters are small (1.0 meter), and the term ($0.5\gamma DN'_\gamma$) provides small values, therefore, it is common to omit this term without introducing significant error. The calculation of N'_q factor as a function of the internal friction angle of the soil, presents numerous proposals, some of which are theoretical and others semi-empirical (Figure 2), see [6-12]; so, the values of the N'_q factor have a wide range for the same angle of internal friction.

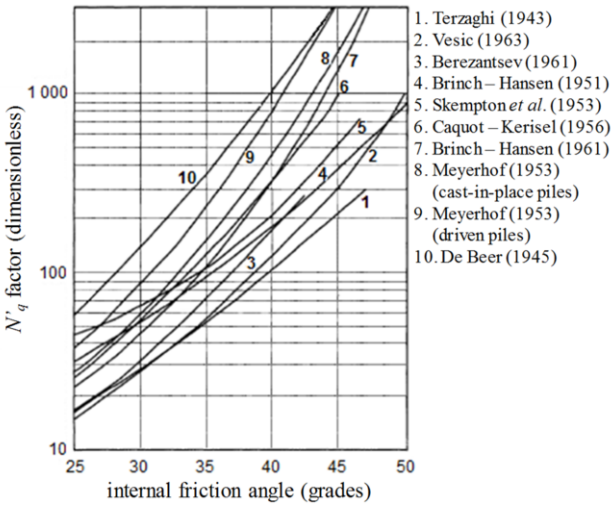

Figure 2. N'_q factor, after [6].

Historically [6-12], various hypotheses have been proposed about the shape and dimensions of the failure surface developed around the pile base, Figure 3 [12], when pile tip receives collapse load. It should be noted that previously shaft resistance has been exceeded. In this case, it is important that support layer must have high strength and sufficient thickness under the tip pile to develop the failure mechanism.

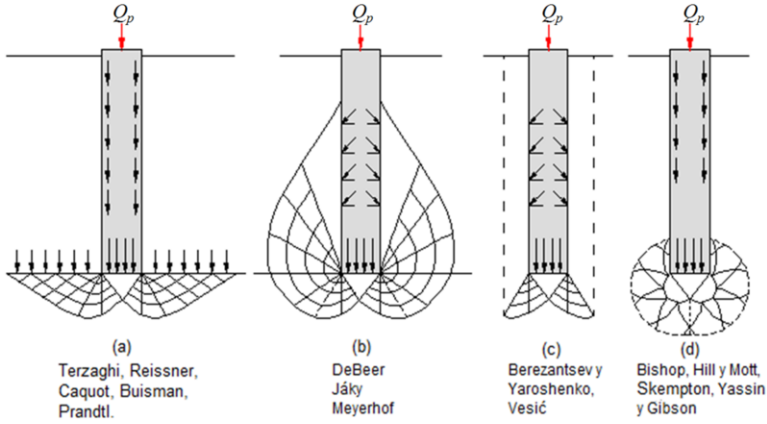

Figure 3. Failure mechanisms proposed by several authors, modified from [12].

The aim of this article is to promote a rational criterion to choose N'_q factor as a function of the internal friction angle (ϕ') of pile tip soil. The N'_q factor analysis considers that hard soil deposit has internal friction angle that varies between 25 and 45 degrees and null cohesion and; weak soil strata with null internal friction angle and cohesion non-zero. Therefore, this study focuses on determining the ultimate load capacity provided by pile tip and evaluating the relationship between Q_p and factor N'_q.

2. Numerical analysis

The numerical analysis realized is with finite element method, see [13,14]. The analysis considers triangular elements of 15 nodes and 12 Gaussian points. The model is axisymmetric due to circular shape of considered pile, Figure 4a shows a mesh example. The parametric analysis considers several effective embedding depths (L_b), from zero to three pile diameters. Each embedding depth requires a particular numerical model. The analysis includes the evaluation of the number of nodes to define the shape of the finite element mesh that does not affect the results of the numerical analysis; from 20,000 nodes there is no change in the results.

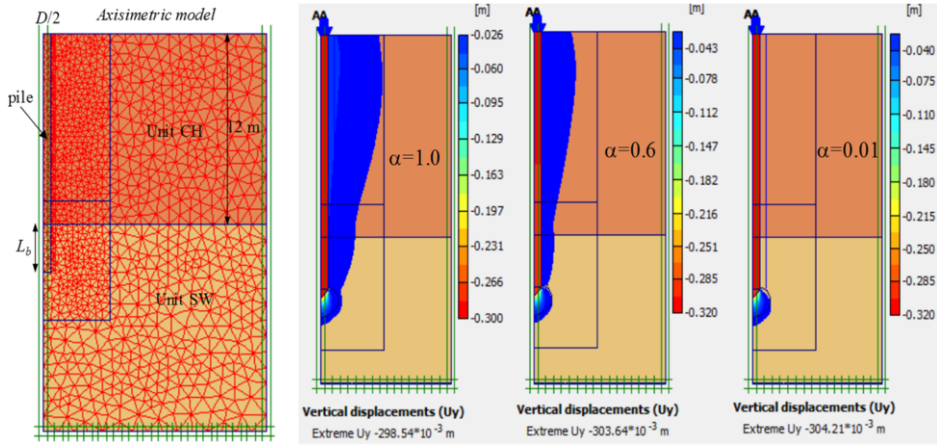

a) b)

Figure 4. a) Numeric model example and b) failure mechanisms by vertical displacement contours.

2.1. Stratigraphy and constitutive models

The constitutive model of the soils is elastoplastic with Mohr-Coulomb failure criterion and pile constitutive model is linear elastic. The pile and soil are modeling with solid elements. The soil-pile_shaft interface is considered to evaluate shaft strength; the computer program provides a tool that reduces in percentage (indicated by the user) soil resistance, and it is associated to interface resistance.

The analysis considers a type stratigraphy: cohesive soil that overlies granular material, sand. Geotechnical design parameters are indicated in the Table 1. The clay parameters are total stresses, by soil low permeability, and to sand deposit, parameters consider effective stresses. The pile tip is support in sand deposit.

Pile diameters considered are 0.6, 0.8 and 1.0 m and pile lengths, between 12 and 15 m. In all cases, pile volumetric weight, γ_c = 24 kN/m^3, and it is compensated by the excavated soil. The pile deformation modulus, E_c = 14,000 (f'c)$^{0.5}$ = 2.170 x 10^7 kPa, for f'c = 250 kg/cm^2, and the pile Poisson ratio considered is 0.20.

Table 1. Geotechnical design parameters of subsoil.

Unit	Depth m	γ_s kN/m^3	ϕ' degree	c_u kPa	E_s kPa	υ ---	Material type
CH	0.0 – 12.0	14.7	0.0	50.0	5,000.0	0.35	undrained
SW	12.0 – 25.0	19.6	25 - 45	0.0	27.000.0	0.30	drained

Note: γ_s: volumetric weight; ϕ': internal friction angle; c_u: cohesion; E_s: deformation modulus; υ: Poisson ratio; CH: high plasticity clay layer; SW: well-graded sand deposit.

2.2. Analysis steps

1. Geostatic stresses, initial conditions due to soil weight and subsoil hydraulic conditions. Resting earth pressure coefficient is 0.5 (for both strata: CH and SW), the groundwater level is at the bottom of the numerical model (zero pore pressure).
2. Pile installing and at the same time, large load is applied to pile head to reach pile collapse. The failure mechanism shape and collapse load value are evaluated.

3. Interpretation of results

3.1. Interface evaluation, α

The adherence coefficient of the soil-pile_shaft interface (α) varies from 0.01, 0.6 and 1.0. To D = 1.0 m and L_b = 3.0 m, Figure 4b shows the vertical displacement contours of the soil adjacent to the pile of three cases of interface analysis: to α = 0.01, null alteration of soil next to the pile and interface resistance is practically null and its input is minimal to calculate tip capacity and numerical calculation time is reduced. The curves for α = 0.6 and 1.0 (Figure 5b) are same to described by Kulhawy (pile head curve of Figure 1a). The curve for α = 0.01 only has the section that corresponds almost totally to the resistance at pile tip.

3.2. Criterions to determine Q_p y N'_q

A necessary condition to calculate the pile tip resistance Q_p, is that the soil-pile_shaft interface resistance is plasticized and does not provide resistance to pile penetration. To fulfill the above, is necessary to calculate Q_s with Equation 2 (theoretical), for α coefficient used in numerical analysis and calculate $Q_p = Q_u - Q_s$. Once Q_p has been calculated, the criterion to define the N'_q factor is: Total volume of failure mechanism, Figure 5a, directly determines the N'_q factor value, this consideration is based on the fact that the term ($0.5\gamma D N'_\gamma$) of Equation 3 is not considered in the professional practice of analysis and geotechnical design of piles. The N'_q factor is:

$$N'_q = \frac{Q_p}{\gamma D_f A_s} \tag{4}$$

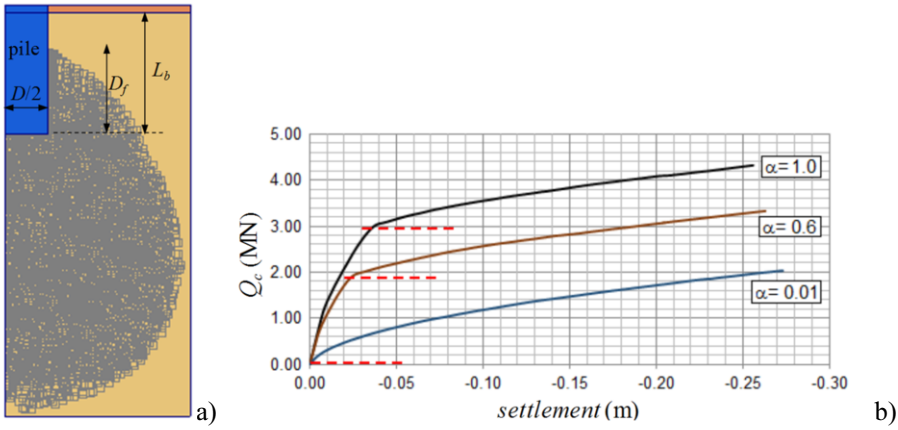

Figure 5. a) Failure mechanism and b) Curves Qc – settlement, results of the evaluation of the interface α.

3.3. Effective embedment depth, L_b

The analysis considers D = 0.6, 0.8 and 1.0 m. Table 2 shows L_b/D ratios considered, where L is defined, the same table indicates that there are four L_b for each D. For L_b = 0, L = 12 m, from this case, L increases as L_b increases. To calculate Q_s with Equation 2 (theoretical), of the stratum CH: c_u= 50 kPa (undrained cohesion, Table 1), α= 0.01 and L= 12 m. The ϕ' parameter considered of SW stratum is 30 degrees.

Figure 6 shows the failure mechanisms defined by the points plasticized by shear stresses, to pile analyzes with a diameter of 1.0 m and effective embedment depths considered. To L_b of 1, 2 and 3 m the shape of the failure mechanism is similar to an elongated spheroid in the long of the pile, and for L_b = 0, it is a less elongated spheroid and very similar to that defined by Skempton (Figure 3d). All failure mechanisms with $L_b/D > 1$, contain resistance supply of soil adjacent to the pile tip and of base soil of pile tip; that is, they include the effect of the factors N'_q and N'_γ. For L_b/D = 0, only there is resistance supply of base soil of pile tip (N'_γ).

Based on calculated Q_p (Table 2), Figure 7 shows the variation of Q_p as a function of L_b/D ratio, and to $L_b/D \geq 2$, Q_p is practically constant. Embedment greater than 2 pile diameters are not efficient.

Table 2. Parametric analysis cases, effective embedment depth, L_b.

D m	L_b/D ratio	L_b m	L m	Identification	Q_u kN	Q_s kN	Q_p kN
1.0	3.0	3.0	15.0	P-1.0-15.0	2,061.3	18.5	2,042.8
	2.0	2.0	14.0	P-1.0-14.0	1,989.1	18.5	1,970.6
	1.0	1.0	13.0	P-1.0-13.0	1,946.7	18.5	1,928.2
	0.0	0.0	12.0	P-1.0-12.0	1,852.7	18.5	1,834.2
0.8	3.0	2.4	14.4	P-0.8-14.4	1,361.7	14.8	1,346.9
	2.0	1.6	13.6	P-0.8-13.6	1,325.3	14.8	1,310.5
	1.0	0.8	12.8	P-0.8-12.8	1,306.5	14.8	1,291.7
	0.0	0.0	12.0	P-0.8-12.0	1,185.9	14.8	1,171.1
0.6	3.0	1.8	13.8	P-0.6-13.8	849.4	11.1	838.3
	2.0	1.2	13.2	P-0.6-13.2	815.4	11.1	804.3
	1.0	0.6	12.6	P-0.6-12.6	800.1	11.1	789.0
	0.0	0.0	12.0	P-0.6-12.0	712.3	11.1	701.2

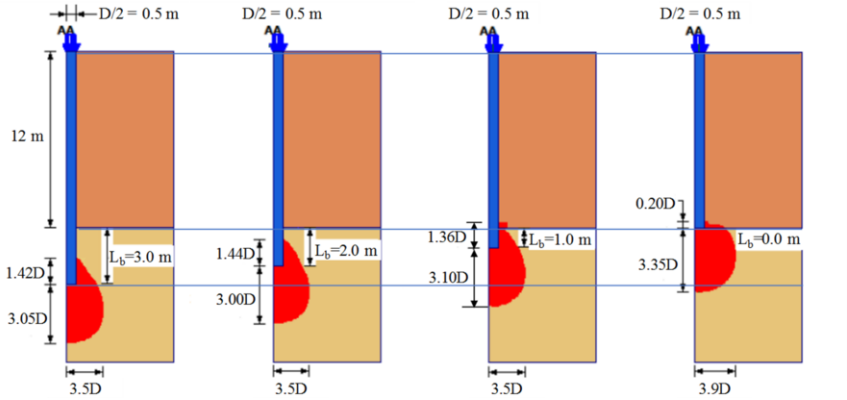

Figure 6. Failure mechanisms by plasticized points by shear stresses, D = 1.0 m.

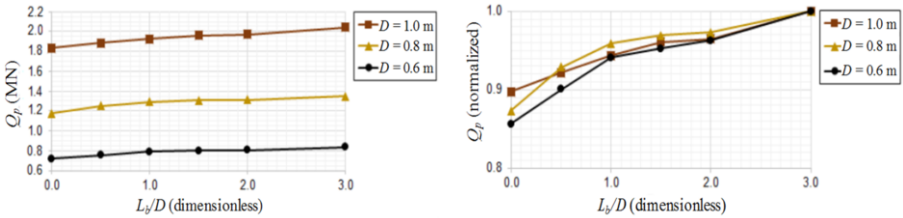

Figure 7. Failure mechanisms by shear stresses plasticized points, D = 1.0 m.

3.4. Evaluation and comparison of N'q factor

Considerations: The internal friction angle (ϕ) of SM unit (Table 1) varies of 25 to 45 degrees. The soil cohesion of SM unit is null, that $L_b/D = 3$ and $D = 1.0$ m.

Figure 8c shows the variation of N'_q as a function of the internal friction angle of the soil that confines the tip of the pile. The factor N'_q varies between 29.7 and 529.0 for ϕ' from 25 to 45 degrees, respectively. This curve occupies an intermediate position in the theoretical values of this factor; the curve is similar to the results reported by Skempton *et al*. (1953). It should be noted that the failure mechanism monitored in the present study is similar to that proposed by Skempton, see Figures 8a and 8b. Table 3 shows the summary of the factors N'_q calculated.

4. Conclusions

The N'_q factor of load capacity of pile tip includes both, the contribution of shear strength of the base pile tip and the adjacent soil too pile tip, zone defined as effective embedment depth. Under this consideration, the N'_q factor depends on the internal friction angle of the support soil of the pile tip, the effective embedment depth and the volumetric weight of the material that the effective embedment offers.

The optimum effective embedment depth is between 2 and 3 diameters of an isolated pile.

The failure mechanism determined in the present study is similar to that reported by Skempton.

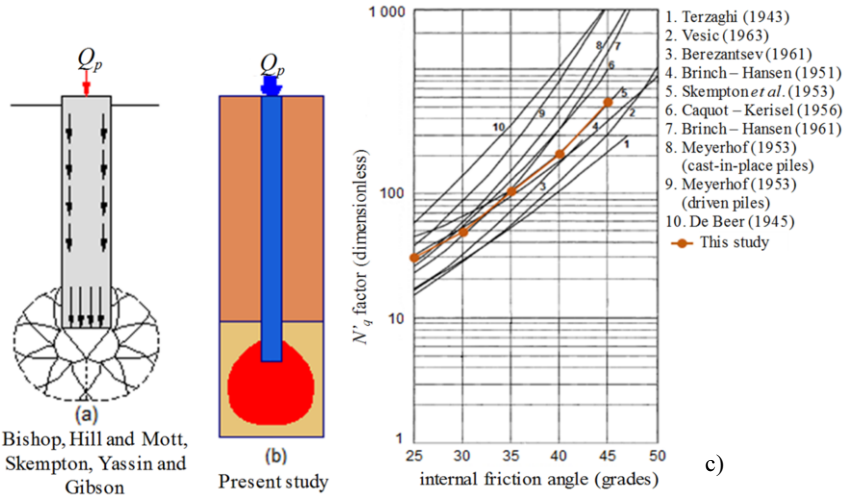

Figure 8. a-b) Failure mechanisms, comparation and c) Evaluation of the N'_q factor.

Table 3. Summary of the factors $N'q$ calculated.

ϕ° degree	25	30	35	40	45
O_n kN	549.0	883.0	1,866.7	3,727.3	9,781.8
N'_q ---	29.7	47.8	101.0	201.6	529.0

References

[1] S. Gourvenec, Effect of embedment on the undrained capacity of shallow foundations under general loading. Géotechnique 58 (2008), No. 3, pp. 177-185.
[2] H. Taiebat and J.P. Carter, Numerical studies of the bearing capacity of shallow foundations on cohesive soil subjected to combined loading. Géotechnique 50 (2000), No. 4, pp. 409-418.
[3] D. Reséndiz, Aplicación del análisis límite al cálculo de la capacidad de carga de cimentaciones, Tesis de licenciatura, Facultad de Ingeniería, Universidad Nacional Autónoma de México, México, p.56, 1961.
[4] F.H. Kulhawy Foundation Engineering Handbook, 14 Drilled Shaft Foundations, Edited by H.Y. Fang, Springer, Boston, MA, 1991.
[5] S. Prakash and H.D. Sharma, Pile Foundations in Engineering Practice, John Wiley & Sons, Inc., New York, 1990.
[6] A. Kezdi, Foundation Engineering Handbook, Pile Foundations, Edited by H.F. Winterkorn and H.Y. Fang, Van Nostrand, New York, 1975.
[7] K. Terzaghi, Theoretical soil mechanics, John Wiley and Sons, New York, 1943.
[8] G.G. Meyerhof, The Ultimate Bearing Capacity of Foundations, Geotechnique, Vol 2 (1951), pp 301-332.
[9] A.W. Skempton, A.S. Yassin and R.E. Gibson, Theorie de la force portente des pieux, Annales de L'Institute Technique Du Batiment Et Des Travaux Publics, Vol. 6, Nos. 63-64, 1953, pp. 285-290.
[10] V.G. Berezantsev, et al., Load bearing capacity and deformation of piled foundations, Proceedings of the 5th International Conference, ISSMFE, Paris, Vol. 2, 1961, pp. 11–12.
[11] A.S. Vesic, Bearing capacity of deep foundations in sand, Highway Research Record, No. 39, Highway Research Board, Washington D. C., 1963.
[12] A.S. Vesic, A study of bearing capacity of deep foundations, Final Report, School of Civil Engg., Georgia Inst. Tech., Atlanta, U.S.A, 1967.
[13] D.M. Potts and L. Zdravkovic, Finite element analysis in geotechnical engineering, theory, Thomas Telford, London, 1999.
[14] D.M. Potts and L. Zdravkovic, Finite element analysis in geotechnical engineering, application. Thomas Telford, London, 2001.